Retromer deficiency observed in Alzheimer's disease causes hippocampal dysfunction, neurodegeneration, and Aβ accumulation

Alim Muhammad*, Ingrid Flores*, Hong Zhang*†, Rui Yu*, Agnieszka Staniszewski*†, Emmanuel Planel*†, Mathieu Herman*†, Lingling Ho‡, Robert Kreber‡, Lawrence S. Honig*§, Barry Ganetzky‡¶, Karen Duff*†, Ottavio Arancio*†, and Scott A. Small*§¶

*Taub Institute for Research on Alzheimer's Disease and the Aging Brain, and Departments of §Neurology and †Pathology, Columbia University College of Physicians and Surgeons, New York, NY 10032; and ‡Laboratory of Genetics, University of Wisconsin, Madison, WI 53706-1580

Contributed by Barry Ganetzky, March 13, 2008 (sent for review December 2, 2007)

Although deficiencies in the retromer sorting pathway have been linked to late-onset Alzheimer's disease, whether these deficiencies underlie the disease remains unknown. Here we characterized two genetically modified animal models to test separate but related questions about the effects that retromer deficiency has on the brain. First, testing for cognitive defects, we investigated retromer-deficient mice and found that they develop hippocampal-dependent memory and synaptic dysfunction, which was associated with elevations in endogenous Aβ peptide. Second, testing for neurodegeneration and amyloid deposits, we investigated retromer-deficient flies expressing human wild-type amyloid precursor protein (APP) and human β-site APP-cleaving enzyme (BACE) and found that they develop neuronal loss and human Aβ aggregates. By recapitulating features of the disease, these animal models suggest that retromer deficiency observed in late-onset Alzheimer's disease can contribute to disease pathogenesis.

flies | mice | pathophysiology

An abnormal elevation in Aβ peptide is thought to represent a neurotoxic agent in Alzheimer's disease (1, 2). Aβ is produced when its parent protein, the amyloid precursor protein (APP), is sequentially cleaved by two enzymes, first by BACE (β-site APP-cleaving enzyme) and then by the multimeric γ-secretase. APP and BACE are transmembrane proteins, and in the last few years many of the molecular mechanisms that regulate the sorting of APP and BACE through membrane compartments of the cell have been elucidated (3). Among these, retromer sorting is a pathway recently implicated in late-onset Alzheimer's disease (LOAD) (4–7). First described in yeast, the retromer sorting pathway consists of a multimeric retromer complex—comprising VPS35, VPS26, VPS29, VPS5, and VPS17—and retromer-binding receptors, in particular VPS10 (8) (Fig. 1*a*). Except for VPS17, mammalian homologues of the retromer complex have been identified (9) and are expressed in the brain among other tissue types. Mammals express a family of VPS10-containing molecules (10), and to date two members of this family, sorLA (5, 7) and sortilin (11), have been shown to act as retromer-binding receptors.

Three lines of evidence have implicated the retromer sorting pathway in LOAD. First, elements related to this pathway are deficient in the brains of LOAD patients, including VPS35, VPS26, and the VPS10-containing receptor sorLA (4). Second, down-regulating any of these three elements in cell culture causes abnormal elevation of Aβ (5, 7). Third, genetic variations in sorLA have been linked to LOAD (7).

Although implicated in LOAD, it is unknown whether deficiencies in the retromer sorting pathway cause key features of the disease. We set out to address this issue by investigating two retromer-deficient animal models, with each model addressing separate but related questions. Because Aβ is produced in LOAD brains that express nonmutated APP, BACE, and γ-secretase, it was important to investigate retromer deficiency on a nonmutated genetic background. To determine whether retromer deficiency causes hippocampal dysfunction, a key clinical feature of Alzheimer's disease, we began by investigating retromer deficiency in genetically modified mice. Our results suggest that retromer deficiency causes hippocampal dysfunction by elevating concentrations of endogenous Aβ peptide.

Although APP and BACE are highly homologous across species, important sequence differences do exist, and these differences can affect their intracellular transport, APP processing, and the neurotoxicity of APP end products (12). Thus, guided by our first series of findings, it became important to investigate the effect that retromer deficiency has on a model brain expressing both human wild-type APP and human wild-type BACE. Exploiting the relative ease of modifying the *Drosophila* genome, we turned to flies in our second series of studies, showing that retromer deficiency increases human Aβ levels and leads to neurodegeneration.

Results

Retromer Deficiency Causes Hippocampal-Dependent Memory and Synaptic Dysfunction. A range of behavioral, imaging, and histological studies have established that hippocampal dysfunction is a dominant clinical feature of Alzheimer's disease (13–15). To test whether retromer deficiency causes hippocampal dysfunction we examined genetically engineered mice. First, extending studies in nonneuronal cell lines (7, 11), we performed coimmunoprecipitation experiments in extracts from mouse brain to show that sorLA and sortilin bind VPS35, confirming that they are neuronal retromer-binding receptors (Fig. 1*a*). By exploring anatomical expression maps (16), we find that genes related to the retromer complex, including VPS26 and VPS35, are highly and differentially expressed in the hippocampal formation [supporting information (SI) Fig. S1]. In contrast, sortilin and sorLA are diffusely expressed throughout the brain. This observation suggests that, within the retromer sorting pathway, molecules related to the retromer complex might confer hippocampal vulnerability.

To test this hypothesis, we investigated VPS26 heterozygote knockout (KO) mice that, in contrast to homozygote KO mice, survive into adulthood and do not manifest gross developmental abnormalities (17). Western blot analysis confirmed that VPS26

Author contributions: L.S.H., B.G., K.D., O.A., and S.A.S. designed research; A.M., I.F., H.Z., R.Y., A.S., E.P., M.H., L.H., R.K., B.G., and S.A.S. performed research; S.A.S. contributed new reagents/analytic tools; A.M., L.H., B.G., K.D., and O.A. analyzed data; and B.G., K.D., O.A., and S.A.S. wrote the paper.

The authors declare no conflict of interest.

Freely available online through the PNAS open access option.

¶To whom correspondence may be addressed. E-mail: ganetzky@wisc.edu or sas68@columbia.edu.

This article contains supporting information online at www.pnas.org/cgi/content/full/0802545105/DCSupplemental.

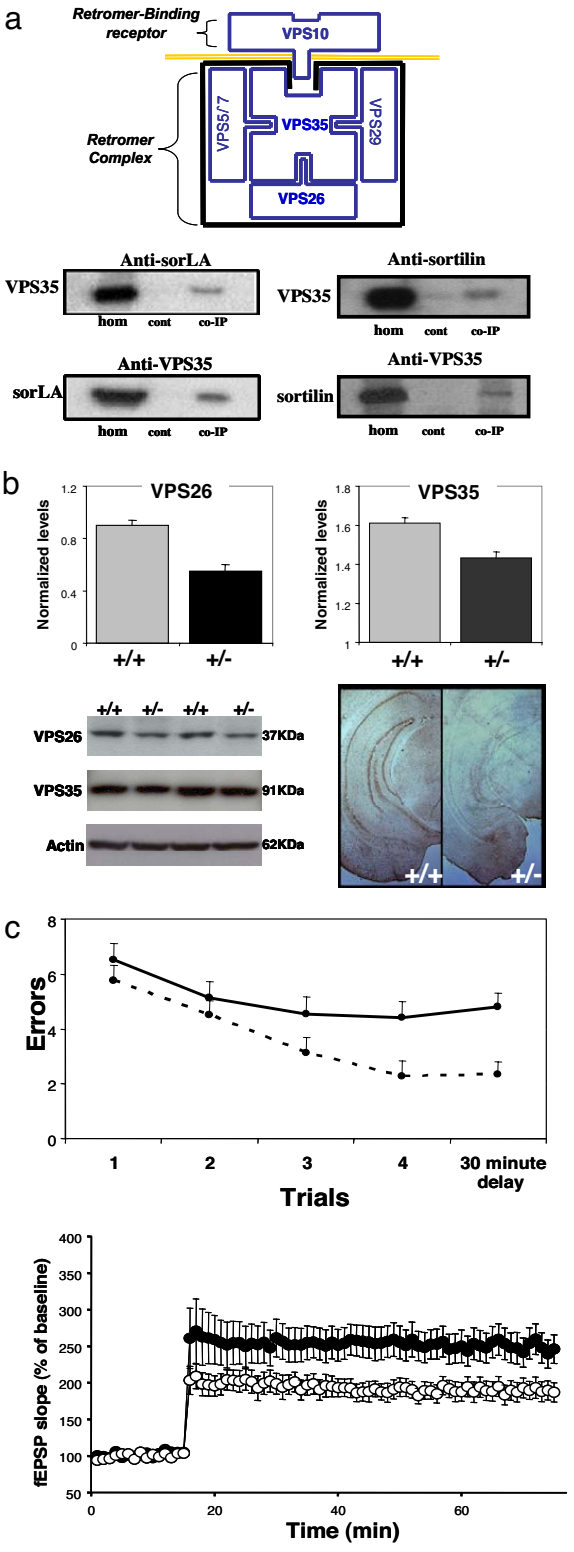

Fig. 1. Retromer deficiency causes hippocampal-dependent memory and synaptic dysfunction. (*a*) (*Top*) The retromer sorting pathway, as first described in yeast, is made up of a multimeric retromer complex, including VPS35 and VPS26, and a retromer-binding receptor, VPS10. (*Middle* and *Bottom*) SorLA and sortilin are VPS10-containing receptors that coimmunoprecipitate with VPS35 in the mouse brain. hom, homogenate; cont, no primary antibody control; co-IP, coimmunoprecipate. (*b*) Retromer-deficient mice, VPS26 heterozygote KO mice (+/−), have diminished brain levels of VPS26 and VPS35, as shown in bar graphs representing mean levels (normalized to actin) measured from the brains of five +/− and five wild-type (+/+) mice. Immunoblots (***Lower Left***) and immunocytochemistry (*Lower Right*) are shown for individual examples. (*c*) Retromer-deficient mice have defects in hippocampal-dependent memory, as measured in the radial-arm water maze (*Upper*). The mean number of errors (*y* axis) are shown for retromer-deficient mice (solid line, +/−) and for wild-type littermates (stippled line, +/+) measured every 90 s during the first four trials and then after a 30-min delay. Retromer-deficient mice have defects in long-term potentiation (*Lower*), recorded from acute hippocampal slices (filled circles, +/−; open circles, +/+).

protein levels are reduced in the brains of the heterozygote KO mice (+/−) compared with wild-type littermates (+/+) (five mice per group; $t = 4.1$, $P = 0.001$) (Fig. 1*b*). Furthermore, consistent with previous studies (18) in which a primary reduction in VPS26 causes a secondary reduction in VPS35, VPS35 protein levels were also reduced in the brains of heterozygote KO mice (five mice per group; $t = 2.9$, $P = 0.01$) (Fig. 1*b*). Thus, the retromer-deficient state in the heterozygote KO mice is similar to that observed in the hippocampal formation of LOAD patients (5).

To test for hippocampal-dependent memory deficits we used the modified radial-arm maze, a behavioral task used to assess the hippocampal formation in other mouse models of Alzheimer's disease (19). Compared with wild-type littermates, the performance of the retromer-deficient mice was found to be defective [18 +/+ and 15 +/− mice; a multivariate test revealed a global effect ($F = 5.6, P = 0.025$) whereas univariate tests revealed that the effect was driven by defects at time 4 ($P = 0.014$) and time 5 ($P = 0.001$)] (Fig. 1*c*). In contrast, both heterozygous KO mice and wild-type mice performed similarly in a visible platform task indicating normal motor, sensory, and motivational capabilities.

Memory defects observed in LOAD correlate with histological markers of hippocampal synaptic dysfunction (20), and a range of recent studies suggest that synaptic dysfunction is an early hallmark of the disease (21, 22). Accordingly, we used electrophysiological techniques to investigate hippocampal synaptic integrity of retromer-deficient mice. Compared with wild-type littermates, heterozygous KO mice were found to have significant defects in long-term potentiation (18 +/+ and 16 +/− mice; $F = 5.1$, $P = 0.025$) (Fig. 1*c*) with preserved paired-pulse facilitation and basal synaptic transmission.

Retromer Deficiency Elevates Levels of Endogenous Aβ in the Mouse Brain. The hippocampal-dependent memory dysfunction observed in LOAD correlates with elevated levels of soluble, not insoluble, forms of the Aβ peptide (21), and it is generally acknowledged that soluble forms of Aβ are neurotoxic. Compared with wild-type littermates, heterozygous KO mice were found by ELISA to have elevated brain levels of endogenous Aβ40 (16 mice per group; $F = 11.4$, $P = 0.002$) and Aβ42 ($F = 8.6$, $P = 0.007$) (Fig. 2*a*). No difference in the level of full-length APP was observed (Fig. 2*b*). To establish a stronger link between the observed elevation in Aβ and hippocampal dysfunction we replicated the electrophysiological studies and found that perfusing the slices with the γ-secretase inhibitor L-685,458 rescued the LTP defects observed in the heterozygous KO mice (five +/+ and six +/− L-685,458-treated mice; $F = 0.03$) (Fig. 2*c*).

The elevation of both Aβ40 and Aβ42 observed in the retromer-deficient mice is characteristic of the profile observed in LOAD (21), and as predicted by this profile a growing number of studies are reporting an up-regulation of BACE activity (as reviewed in ref. 23). BACE cleaves APP into sAPPβ and CTFβ, the membrane-bound C-terminal fragment that contains the Aβ sequence. γ-Secretase then cleaves CTFβ to liberate the Aβ peptide. In secondary analyses, we explored the profile of intermediate APP end products to assess which cleavage step is most affected by retromer deficiency. Compared with wild-type littermates, levels of sAPPβ, but not sAPPα, were found to be elevated in the heterozygote KO mice, suggesting that retromer dysfunction increases

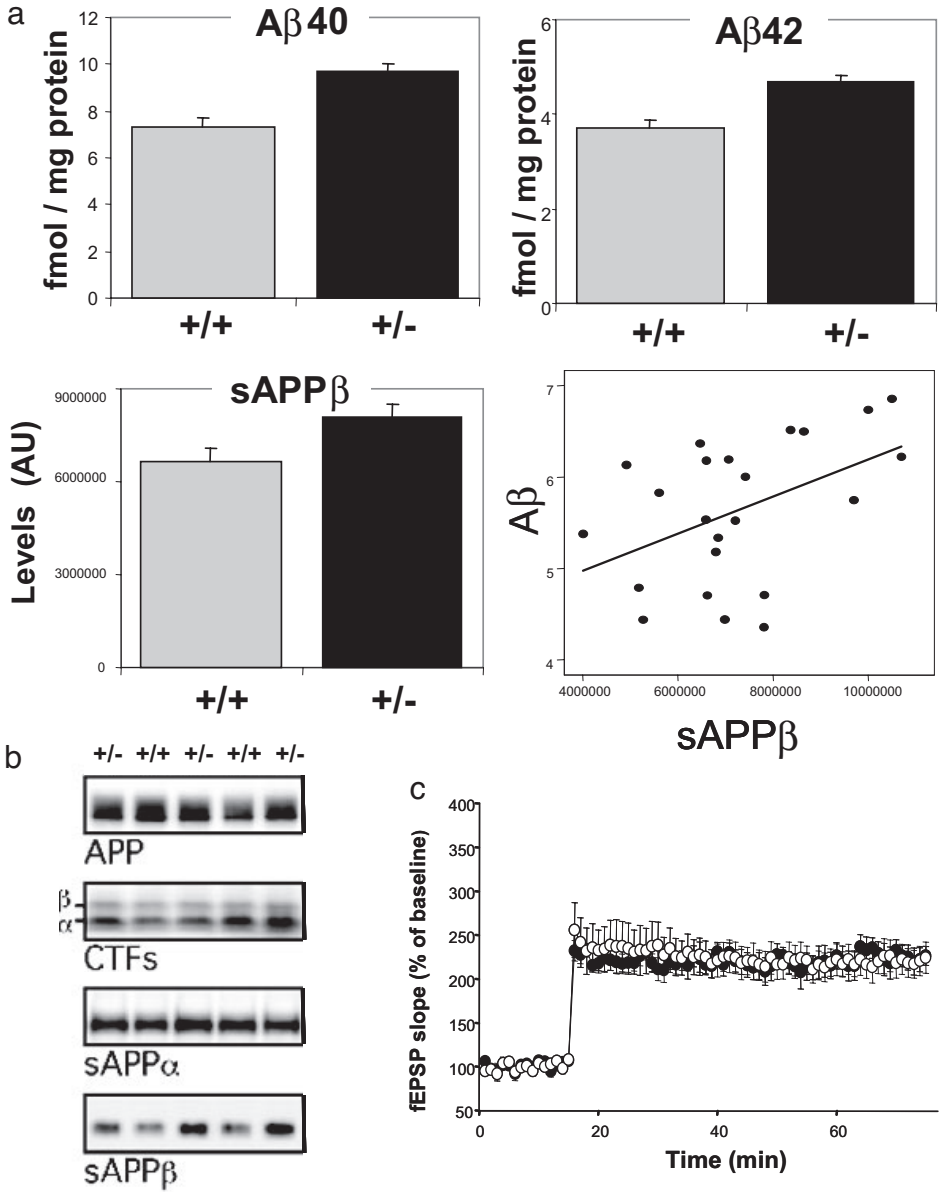

Fig. 2. Retromer deficiency elevates levels of endogenous Aβ in the mouse brain. (*a*) Retromer-deficient mice (+/−) have elevated levels of endogenous Aβ40 and Aβ42 (*Upper*, measured in 16 +/− and 18 +/+ mice). Retromer-deficient mice (+/−) have elevated levels of endogenous sAPPβ (*Lower Left*). Levels of sAPPβ and Aβ are significantly correlated (*Lower Right*). (*b*) Immunoblots from the brains of three retromer-deficient mice (+/−) and two wild-type littermates (+/+) show that, except for sAPPβ, no differences were observed for full-length APP, CTFs, or sAPPα. (*c*) Administration of the γ-secretase inhibitor L-685,458 rescues the LTP defects in retromer-deficient mice (filled circles, +/−; open circles, +/+).

BACE activity (24) (12 mice per group; $F = 4.9$, $P = 0.038$) (Fig. 2*a*). CTFβ levels, however, were not significantly elevated in the retromer-deficient mice (Fig. 2*b*), suggesting that the mild increase in CTFβ fragments induced by retromer deficiency might be fully cleaved by γ-secretase. This interpretation is supported by our observation that sAPPβ and averaged Aβ levels were significantly correlated among individual mice ($\beta = 0.47$, $P = 0.027$) (Fig. 2*a*). Nevertheless, we have not excluded the possibility that retromer deficiency acts by decreasing clearance or stabilizing sAPPβ or another APP end product.

Retromer Deficiency Elevates Levels of Human Aβ in the Fly Brain and Causes Neurodegeneration. Although highly homologous across species, murine APP and BACE have important sequence differences from their human counterparts that affect the cell biology of APP and BACE and the toxicity of APP end products (12). Therefore, we examined the effect of retromer deficiency in animals that express both human wild-type APP and human BACE. Because of the difficulty in engineering the complex genotype in mice, a *Drosophila* Alzheimer's disease model (25) in which human wild-type APP and BACE are expressed using the *GAL4/UAS* system (26) was used. *UAS-APP* and *UAS-BACE* were driven ubiquitously by using an actin-GAL4 (*Act-GAL4*) driver. These flies were crossed to line *DfVPS35*, which has a deletion in the *Drosophila VPS35* ortholog. Sibling flies were *ACT-GAL4*, *UAS-APP*, and *UAS-BACE* and carried either two copies of *VPS35* (+/+) or just one (+/−), enabling us to investigate the phenotypic consequences of reducing retromer expression by 50%.

To test whether retromer deficiency affects APP processing, Western blot analysis revealed that, compared with +/+ flies, the

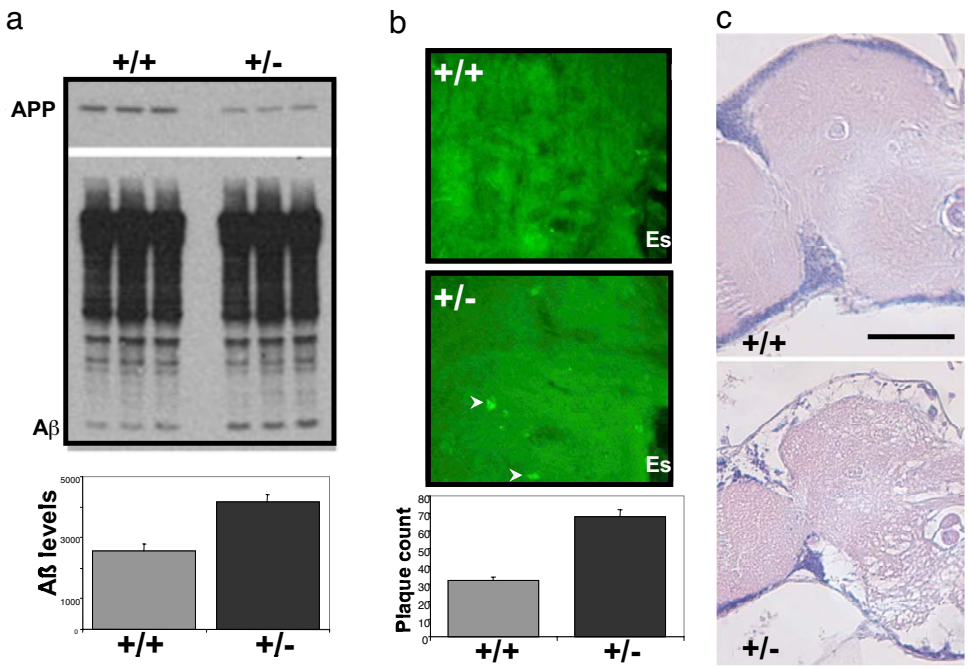

Fig. 3. Retromer deficiency elevates levels of human Aβ in the brains of flies expressing human APP and BACE and causes neurodegeneration. (*a*) Retromer-deficient flies (+/− for VPS35) expressing human APP and human BACE have elevated brain levels of human Aβ compared with control flies (+/+ for VPS35) expressing human APP and human BACE. Immunoblots in *Upper* show individual examples (note reduction in full-length APP), and the bar graph in *Lower* shows means levels from 10 flies per genotype. (*b*) High-magnification view of frontal brain sections at approximately midbrain from control (+/+) and retromer-deficient (+/−) flies expressing human APP and human BACE stained with 4G8 antibody to detect Aβ deposits (arrowheads). These deposits are larger and more numerous in the retromer-deficient flies. Each section shows a portion of the central neuropil located to the left and adjacent to the esophagus (Es). Anterior is toward the top. (*c*) Frontal brain sections at the midbrain level shown for control (+/+) and retromer-deficient (+/−) flies expressing human wild-type APP and human BACE. The left half of the central brain and optic lobe are shown. Esophagus is in the middle of the section at the right margin. Extensive neurodegeneration can be seen in the neuropil of retromer-deficient flies. (Scale bar: 50 μm.)

+/− flies had elevated levels of human Aβ peptide ($t = 4.8$, $P = 0.009$) (Fig. 3*a*). Moreover, immunocytochemistry using anti-Aβ antibodies revealed that, compared with +/+ flies, the +/− flies had greater deposition of Aβ aggregates ($t = 6.2$, $P = 0.001$) (Fig. 3*c*). Aβ accumulation was associated with a substantial reduction in lifespan in +/− compared with +/+ flies (7 days vs. 16 days at 50% survivorship) and more severe manifestation of a defect in wing vein development (25) (Fig. S2) and, most importantly, was associated with extensive neurodegeneration throughout the central brain (Fig. 3*c*). At least 50% of the +/− flies showed clear evidence of neurodegeneration, and a significant fraction showed dramatic loss of brain tissue. In contrast, the incidence and the severity of neurodegeneration in +/+ flies were far less. Only ≈10% of these flies showed any indication of neurodegeneration, and no flies manifested the extreme tissue loss that was found regularly in the +/− flies. These phenotypes are due to loss of *VPS35*, because comparable results were observed in flies in which *DfVPS35* was replaced by a *UAS-RNAi* construct that specifically reduced *VPS35* expression.

Discussion

Developing and characterizing animal models that express molecular defects found in early-onset Alzheimer's disease is one of the major achievements in the field (27, 28). Nevertheless, the defects in APP or presenilins observed in early-onset Alzheimer's disease do not exist in LOAD, the form of the disease accounting for >95% of all cases. Thus, developing animal models that express molecular defects found in LOAD, on the background of nonmutated APP and presenilin, has emerged as an important goal. With this in mind, we have exploited the strengths provided by different animal models to address complementary questions about the retromer-deficient state observed in LOAD. Taken together, our findings show that deficiencies in the retromer sorting pathway can cause hippocampal dysfunction, neurodegeneration, and Aβ accumulation. By establishing that retromer-deficient animals recapitulate a number of LOAD features, these findings contribute to the growing body of evidence implicating the retromer sorting pathway in the pathogenesis of the disease.

APP is a transmembrane protein that is actively sorted through many membrane compartments of the cell, and sorLA has been shown to act in APP sorting (6, 29). Extending previous studies (7), we find that sorLA is a binding receptor of the neuronal retromer complex. Mechanistically this suggests that deficiencies in VPS26 and VPS35 accelerate Aβ production by increasing the resident time of APP within a given membrane compartment, thereby increasing its colocalization with BACE and accelerating β-cleavage. Future studies are required to test this proposed cellular mechanism, but it can account for why levels of both Aβ40 and Aβ42 are typically increased in the brains of LOAD patients even in the absence of defects in APP or BACE.

Anatomically, the differential expression pattern of VPS35 and VPS26 suggests that it is the retromer complex itself, not the retromer-binding receptors, that impose the regional vulnerability of defects in this sorting pathway. More generally, understanding why the hippocampal formation differentially expresses retromer complex molecules might provide insight into disease-related regional vulnerability. In this regard, it is interesting that numerous recent studies have shown that the retromer complex plays a role in wnt signaling (as reviewed in ref. 30), a morphogenic pathway that is influenced by presenilin (31) and that has been genetically implicated in LOAD (32). The hippocampal formation, and in particular the entorhinal cortex (33), have a number of distinct morphogenic features, and future studies are required to test the hypothesis

that retromer–wnt interactions support the morphogenic complexity of the hippocampal formation, thereby predisposing this structure to LOAD pathogenesis.

As in other animal models of disease, retromer-deficient mice and flies only partially phenocopy the disease itself. We are currently aging our colony of retromer-deficient mice to test whether these mice develop amyloid plaques, cell loss, or abnormal tau hyperphosphorylation. Even as partial models, however, the retromer-deficient animals introduced here can be used to further enhance our cellular and molecular understanding of LOAD and provide *in vivo* models with which to screen pharmacological agents against this devastating and undertreated disorder.

Materials and Methods

Mouse Experiments. ***Genetically modified mice.*** Congenic VPS26 heterozygote KO mice were crossed for 10 generations on a 129/SvEv background and then maintained by brother–sister mating (34). Three- to 6-month-old VPS26 KO and wild-type littermates were used for all experiments.

Western blotting. Mouse brain samples were homogenized in ice-cold buffer, 10 mM HEPES (pH 7.4) containing 0.32 M sucrose, 0.5 mM $CaCl_2$, 1 mM $MgCl_2$, 1 mM AEBSF-HCl (Calbiochem), 3 μg/ml aprotinin, 3 μg/ml pepstatin A, 10 μg/ml leupeptin, and Protease Inhibitor Mixture (Roche). After centrifugation, $\approx$20 μg of soluble brain proteins were resolved by SDS/PAGE and electrotransferred to PVDF membrane (Bio-Rad). The immobilized blot was briefly soaked in TBS and subsequently in blocking solution: 1:1 Odyssey blocking buffer (LI-COR Biosciences, catalog no. 927-40000) and TBS plus 0.1% Tween 20 overnight. After washing, the blot was immunoreacted with a primary antibody (1:1,000 dilution) in blocking solution for 3 h at room temperature. The images were acquired with the Odyssey Infrared Imaging System (LI-COR Biosciences) at channel 700 and analyzed by the software program as specified in the Odyssey software manual.

Coimmunoprecipitation. Coimmunoprecipitation was performed by using a fraction of mouse brain in a buffer (1% Nonidet P-40/20 mM HEPES, pH 7.4/125 mM NaCl/50 mM NaF/protease inhibitors) as previously described (18), using 5 μg of primary antibody against VPS35, SorLA, and APP antibodies and Tosylactivated Dynabeads M-280 (Dynal).

Cognitive testing. The radial-arm water maze task has been described previously (35). Each day of testing included four consecutive acquisition trials and a fifth retention trial with a 30-min delay after the fourth trial. Each trial lasted 1 min. Errors were counted when the mouse went to an arm without platform or took $>$10 s to enter any arm of the maze. The number of errors in each trial in the last 3 days of testing was averaged and used for statistical analysis.

Electrophysiology. Transverse slices (400 μm) were cut with a tissue chopper (Electron Microscopy Sciences) and maintained in an interface chamber at 29°C for 90 min before recording, as previously reported (35). Briefly, CA1 field excitatory postsynaptic potentials (fEPSPs) were recorded by placing both the stimulating and the recording electrodes in CA1 stratum radiatum. BST was assayed either by plotting the stimulus voltages (V) against slopes of fEPSP or by plotting the peak amplitude of the fiber volley against the slope of the fEPSP to generate input–output relations. After a 15-min baseline in which responses were evoked at an intensity of $\approx$35% of the maximum evoked response, LTP was induced by using a θ-burst stimulation (four pulses at 100 Hz, with bursts repeated at 5 Hz and each tetanus including three 10-burst trains separated by 15 s). In some experiments slices were perfused with the γ-secretase inhibitor L-685,458 at 0.5 μM (for 2 h before applying the θ-burst stimulation). In these experiments the inhibitor did not affect LTP in wild-type slices.

Western blot analysis of APP and its end products. Western blotting was performed as described (36), and soluble species of APP in diethyl acetate extracts were detected with m3.2 antibody (detects sAPPβ; generous gift of Paul Mathews, Nathan S. Kline Institute, Orangeburg, NY) or sAPPβ antibody (Signet Laboratories). Full-length APP and CTFs were detected with C1/6.1 (generous gift of Paul Mathews) on radioimmunoprecipitation assay extracts from frozen tissues (37).

Aβ ELISA. ELISA for murine Aβ 40 and 42 was performed as previously described (38, 39) using diethyl acetate extracts from fresh hemibrains and antibodies from Centocor.

Fly Experiments. ***Genetically modified*** **Drosophila.** We obtained the *UAS-APP/CyO*; *UAS-BACE^{406}/UASBACE^{406}* stock constructed by Greeve *et al.* (25). To delete a copy of *VPS35*, we used *Df(2R)Egfr/CyO* obtained from the Bloomington *Drosophila* Stock Center at Indiana University (Bloomington, IN). Here we refer to this deficiency as *DfVPS35*. We generated a *DfVPS35/CyO; Act-GAL4/TM6* stock through standard crosses. Males from this stock were crossed with *UAS-APP/UAS-APP; UAS-BACE406/UAS-BACE406* females to generate *DfVPS35/UAS-APP; Act-GAL4/UAS-BACE406* and *CyO/UAS-APP; Act-GAL4/UAS-BACE406* siblings. Both sets of offspring express *UAS-APP* and *UAS-BACE* driven by *Act-GAL4*. However, offspring of the former genotype are deleted for one copy of *VPS35* whereas the latter have the normal two doses of this gene. For simplicity, we refer to these two genotypes as +/− and +/+, respectively. Crosses were carried out on standard cornmeal/molasses/agar medium at $\approx$22°C.

Western blot of APP and its end products. Ten brains from each group (double and triple mutant) flies were homogenized with 100 μl of Tricine sample buffer (Bio-Rad) and heated for 3–5 min. After centrifugation the clear supernatant (20 μl for each lane) was loaded on 10–20% Tricine gels (Invitrogen) and resolved by electrophoresis. The blots were probed for APP by using the C/16.1 antibody and for Aβ peptide by using the 6E10 antibody (1:1,000, Signet). The signals were detected as described above.

Histology. Newly eclosed adults were shifted to 25°C and aged for 7–10 days. Heads were dissected and placed in fresh Carnoy's fixative for 24 h at 22°C, washed in 70% ethanol, and processed into paraffin by using standard histological procedures. Serial 6μ frontal sections were taken, stained in hematoxylin and eosin, and examined under a light microscope. To assess plaque load, 4G8 antibody (1:200, Signet) was used to incubate 6μ brain sections overnight at 4°C. To assess plaque load, 4G8 antibody (1:200, Signet) was used to incubate 6-μm-thick brain sections overnight at 4°C. Secondary antibody Alexa Fluor 488 (1:200, Invitrogen) was used for fluorescent staining. Photos were taken by using a SPOT Insight 4Mp 14.2 camera (Diagnostic Instruments) with SPOT Advanced (Spot Software version 4.6; Diagnostic Instruments).

ACKNOWLEDGMENTS. We are grateful to Dr. Rita Reifegerste (University of Hamburg, Hamburg, Germany) for providing transgenic flies; Dr. Paul M. Mathews for the gift of m3.2 and C1/6.1 antibodies; and Dr. Sonia Jung (Centocor), Mr. Kenneth Hess, Ms. Lili Wang for technical help. This work was supported in part by the Alzheimer's Association (S.A.S.); National Institutes of Health Federal Grants AG025161 (to S.A.S.), NS48447 (to K.D.), AG172116 (to K.D.), NS015390 (to B.G.), and NS049442 (to O.A.); and the McKnight Neuroscience of Brain Disorders Award (to S.A.S.).

1. Hardy J, Selkoe DJ (2002) The amyloid hypothesis of Alzheimer's disease: Progress and problems on the road to therapeutics. *Science* 297:353–356.
2. Gandy S (2005) The role of cerebral amyloid beta accumulation in common forms of Alzheimer disease. *J Clin Invest* 115:1121–1129.
3. Small SA, Gandy W (2006) Sorting through the cell biology of Alzheimer's disease: Intracellular pathways to pathogenesis. *Neuron* 52:15–31.
4. Scherzer CR, *et al.* (2004) Loss of apolipoprotein E receptor LR11 in Alzheimer disease. *Arch Neurol* 61:1200–1205.
5. Small SA, *et al.* (2005) Model-guided microarray implicates the retromer complex in Alzheimer's disease. *Ann Neurol* 58:909–919.
6. Andersen OM, *et al.* (2005) Neuronal sorting protein-related receptor sorLA/LR11 regulates processing of the amyloid precursor protein. *Proc Natl Acad Sci USA* 102:13461–13466.
7. Rogaeva E, *et al.* (2007) The neuronal sortilin-related receptor SORL1 is genetically associated with Alzheimer disease. *Nat Genet* 39:168–177.
8. Seaman MN (2005) Recycle your receptors with retromer. *Trends Cell Biol* 15:68–75.
9. Haft CR, *et al.* (2000) Human orthologs of yeast vacuolar protein sorting proteins Vps26, 29, and 35: Assembly into multimeric complexes. *Mol Biol Cell* 11:4105–4116.
10. Hampe W, *et al.* (2001) The genes for the human VPS10 domain-containing receptors are large and contain many small exons. *Hum Genet* 108:529–536.
11. Seaman MN (2004) Cargo-selective endosomal sorting for retrieval to the Golgi requires retromer. *J Cell Biol* 165:111–122.
12. Wang R, *et al.* (1996) The profile of soluble amyloid beta protein in cultured cell media. Detection and quantification of amyloid beta protein and variants by immunoprecipitation-mass spectrometry. *J Biol Chem* 271:31894–31902.
13. Braak H, Braak E (1996) Evolution of the neuropathology of Alzheimer's disease. *Acta Neurol Scand Suppl* 165:3–12.
14. Jacobs DM, *et al.* (1995) Neuropsychological detection and characterization of preclinical Alzheimer's disease. *Neurology* 45:957–962.
15. Fox NC, *et al.* (1998) Presymptomatic cognitive deficits in individuals at risk of familial Alzheimer's disease. A longitudinal prospective study. *Brain* 121:1631–1639.
16. Lein ES, *et al.* (2007) Genome-wide atlas of gene expression in the adult mouse brain. *Nature* 445:168–176.
17. Lee JJ, *et al.* (1992) Identification and characterization of a novel, evolutionarily conserved gene disrupted by the murine H beta 58 embryonic lethal transgene insertion. *Development* 115:277–288.
18. Verges M, *et al.* (2004) The mammalian retromer regulates transcytosis of the polymeric immunoglobulin receptor. *Nat Cell Biol* 6:763–769.
19. Sant'Angelo A, Trinchese F, Arancio O (2003) Usefulness of behavioral and electrophysiological studies in transgenic models of Alzheimer's disease. *Neurochem Res* 28:1009–1015.

20. Masliah E, *et al.* (1994) Synaptic and neuritic alterations during the progression of Alzheimer's disease. *Neurosci Lett* 174:67–72.
21. Lue LF, *et al.* (1999) Soluble amyloid beta peptide concentration as a predictor of synaptic change in Alzheimer's disease. *Am J Pathol* 155:853–862.
22. Mucke L, *et al.* (2000) High-level neuronal expression of abeta 1–42 in wild-type human amyloid protein precursor transgenic mice: Synaptotoxicity without plaque formation. *J Neurosci* 20:4050–4058.
23. Johnston JA, *et al.* (2005) Expression and activity of beta-site amyloid precursor protein cleaving enzyme in Alzheimer's disease. *Biochem Soc Trans* 33:1096–1100.
24. Lee EB, *et al.* (2005) BACE overexpression alters the subcellular processing of APP and inhibits Abeta deposition in vivo. *J Cell Biol* 168:291–302.
25. Greeve I, *et al.* (2004) Age-dependent neurodegeneration and Alzheimer-amyloid plaque formation in transgenic Drosophila. *J Neurosci* 24:3899–3906.
26. Brand AH, Perrimon N (1993) Targeted gene expression as a means of altering cell fates and generating dominant phenotypes. *Development* 118:401–415.
27. Price DL, *et al.* (1998) Alzheimer's disease: Genetic studies and transgenic models. *Annu Rev Genet* 32:461–493.
28. Duff K (2001) Transgenic mouse models of Alzheimer's disease: Phenotype and mechanisms of pathogenesis. *Biochem Soc Symp* 67:195–202.
29. Offe K, *et al.* (2006) The lipoprotein receptor LR11 regulates amyloid beta production and amyloid precursor protein traffic in endosomal compartments. *J Neurosci* 26:1596–1603.
30. Eaton S (2008) Retromer retrieves wntless. *Dev Cell* 14:4–6.
31. Kang DE, *et al.* (2002) Presenilin couples the paired phosphorylation of beta-catenin independent of axin: Implications for beta-catenin activation in tumorigenesis. *Cell* 110:751–762.
32. De Ferrari GV, *et al.* (2007) Common genetic variation within the low-density lipoprotein receptor-related protein 6 and late-onset Alzheimer's disease. *Proc Natl Acad Sci USA* 104:9434–9439.
33. Solodkin A, Van Hoesen GW (1996) Entorhinal cortex modules of the human brain. *J Comp Neurol* 365:610–617.
34. Perkins CP (1993) Further characterization of the murine embryonic lethal mutant Hb58, and its role in the visceral yolk sac. PhD dissertation (Columbia University, New York).
35. Petrone A, *et al.* (2003) Receptor protein tyrosine phosphatase alpha is essential for hippocampal neuronal migration and long-term potentiation. *EMBO J* 22:4121–4131.
36. Noble W, *et al.* (2005) Inhibition of glycogen synthase kinase-3 by lithium correlates with reduced tauopathy and degeneration in vivo. *Proc Natl Acad Sci USA* 102:6990–6995.
37. Planel E, *et al.* (2004) Alterations in glucose metabolism induce hypothermia leading to tau hyperphosphorylation through differential inhibition of kinase and phosphatase activities: Implications for Alzheimer's disease. *J Neurosci* 24:2401–2411.
38. Burns M, *et al.* (2003) Presenilin redistribution associated with aberrant cholesterol transport enhances beta-amyloid production in vivo. *J Neurosci* 23:5645–5649.
39. Schmidt SD, Nixon RA, Mathews PM (2005) ELISA method for measurement of amyloid-beta levels. *Methods Mol Biol* 299:279–297.